ACS APPLIED MATERIALS & INTERFACES

Research Article

www.acsami.org

Pickering Emulsions Prepared by Layered Niobate $K_4Nb_6O_{17}$ Intercalated with Organic Cations and Photocatalytic Dye Decomposition in the Emulsions

Teruyuki Nakato,*[,†] Hiroaki Ueda,[‡] Sachika Hashimoto,[‡] Ryosuke Terao,[‡] Miyuki Kameyama,[‡] and Emiko Mouri[†]

[†]Department of Applied Chemistry, Kyushu Institute of Technology, 1-1 Sensui-cho, Tobata-ku, Kitakyushu-shi, Fukuoka 804-8550, Japan

[‡]Graduate School of Bio-Applications and Systems Engineering, Tokyo University of Agriculture and Technology, 2-24-16 Naka-cho, Koganei-shi, Tokyo 184-8588, Japan

Supporting Information

ABSTRACT: We investigated emulsions stabilized with particles of layered hexaniobate, known as a semiconductor photocatalyst, and photocatalytic degradation of dyes in the emulsions. Hydrophobicity of the niobate particles was adjusted with the intercalation of alkylammonium ions into the interlayer spaces to enable emulsification in a toluene–water system. After the modification of interlayer space with hexylammonium ions, the niobate stabilized water-in-oil (w/o) emulsions in a broad composition range. Optical microscopy showed that the niobate particles covered the surfaces of emulsion droplets and played a role of emulsifying agents. The niobate particles also enabled the generation of oil-in-water (o/w) emulsions in a limited composition range. Modification with dodecylammonium ions, which turned the niobate particles more hydrophobic, only gave w/o emulsions, and the particles were located not only at the toluene–water interface but also inside the toluene continuous phase. On the other hand, interlayer modification with butylammonium ions led to the formation of o/w emulsions. When porphyrin dyes were added to the system, the cationic dye was adsorbed on niobate particles at the emulsion droplets whereas the lipophilic dye was dissolved in toluene. Upon UV irradiation, both of the dyes were degraded photocatalytically. When the cationic and lipophilic porphyrin molecules were simultaneously added to the emulsions, both of the dyes were photodecomposed nonselectively.

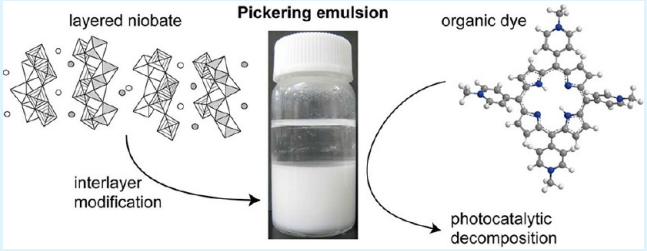

KEYWORDS: *Pickering emulsion, layered niobate, intercalation, adsorption, interface photocatalysis*

INTRODUCTION

Emulsions stabilized by particles, called Pickering emulsions, have been rediscovered and attracted attention in the past decade.[1−5] Solid particles are adsorbed more strongly than conventional surfactants on oil–water interfaces to yield highly stable emulsions. The emulsions provide broad practical applications in various fields such as petroleum, food, cosmetic, and pharmaceutical industries, and are also recognized as a kind of multicomponent soft matter where particles are aggregated in a specific manner at the structured oil–water interface. For the formation of Pickering emulsions, hydrophilic or hydrophobic property of the emulsifier particles, or in other words, wettability, is important.[3−5] Appropriately hydrophobic and hydrophilic particles yield water-in-oil (w/o) and oil-in-water (o/w) emulsions, respectively. The hydrophobicity is usually controlled by surface modification of the particles. Since the surface reaction site for the hydrophobicity modification is not well-defined for conventional spherical particles, precisely controlled surface modification is not easily attained. To overcome this, utilization of Janus particles[6−10] and addition of molecular surfactants have been examined for organizing stable Pickering emulsions.[11−15] However, complicated techniques are required for preparing the emulsifying particles in the former case, and leakage of the surfactants is possible in the latter.

Although spherical particles are usually used as the particle emulsifier of Pickering emulsions, platelike particles can be utilized as alternative emulsifiers. The platy shape has been suggested to be advantageous for the formation of network structures at the water–oil interfaces.[16,17] Because this type of particle morphology is usually observed for layered crystals, Pickering emulsions have been prepared with inorganic layered materials.[16−48] If the layered crystals have ion-exchangeable sites in their interlayer spaces, as observed for numerous layered compounds exemplified by smectite-type clays and layered double hydroxides, the solid emulsifiers have an additional advantage, which is the ease of hydrophobicity

Received: June 3, 2012
Accepted: July 31, 2012
Published: July 31, 2012

   dx.doi.org/10.1021/am300987x | ACS Appl. Mater. Interfaces 2012, 4, 4338–4347

modification by incorporation of organic molecules into their interlayer spaces through ion exchange. The organic species is readily intercalated into sterically defined sites with the amounts determined by the ion exchange capacity, and the intercalation alters the hydrophobicity of the layered crystals.[49] Hence, the ion-exchangeable layered crystals can be utilized as the particle emulsifiers, and the emulsification behavior can be tuned through the hydrophobicity control with the intercalation of appropriate organic ions.

So far, ion-exchangeable layered crystals with and without intercalation of organic molecules have been investigated as the solid emulsifiers. Smectite-type clays form o/w emulsions without intercalation of organic species[16,22,23,45] whereas the clays intercalated with organic cations produce o/w[18,28,42,44] or w/o[19,25] emulsions depending on the organic species. Layered double hydroxides with and without the intercalation of organic substances also stabilize emulsions.[16,23,26,27,32] Phase inversion between o/w and w/o emulsions has also been observed for the emulsification with the organically modified layered materials.[20,32,35,48] However, to the best of our knowledge, investigations that systematically alter the interlayer conditions for the same layered crystal have not been carried out.

Another aspect of the Pickering emulsions is utilization of physicochemical properties of the solid emulsifiers for novel functions of the emulsions. Inorganic emulsifiers can add unusual properties to the emulsions if we use the particles with advanced optic, photochemical, electric, and magnetic properties although many studies have utilized inert solid particles typically exemplified by silica as emulsifiers. Examples are emulsions with magnetic particles responsive to external magnetic fields.[50−53] For the case of ion-exchangeable layered materials, however, the emulsifiers have been limited to physicochemically inert ones such as clay minerals. Although Pickering emulsions of graphene oxide have been reported as a very few exceptions, functions of the obtained emulsions have not been developed.[40,41,43] It should be important to systematically control the emulsifying behavior of physicochemically active layered compounds for designing hierarchically organized functional systems with layered materials based on the emulsion structures.

Here, we report Pickering emulsions prepared with layered hexaniobate $K_4Nb_6O_{17}$ that is a photocatalytically active wide band gap semiconductor[54,55] and is intercalated with organic cations through ion exchange.[56−58] The photocatalytic activity allows decomposition of organic species that is adsorbed on the material or dissolved in the surrounding liquid upon UV irradiation.[59−62] Hydrophobicity of the material is broadly modified by intercalation of alkylammonium ions whereas bare $K_4Nb_6O_{17}$ is hydrophilic.[63−66] We have obtained both w/o and o/w emulsions depending on the intercalated alkylammonium species with different chain length. In addition, the niobate particles located at the water−oil interface photocatalytically decompose dyes dissolved in both oil and water phases.

EXPERIMENTAL SECTION

Preparation of the Alkylammonium-Intercalated Niobates. Tetrapotassium hexaniobate trihydrate $K_4Nb_6O_{17}\cdot 3H_2O$ was prepared by heating a mixture of K_2CO_3 and Nb_2O_5 (2.1: 3.0 in molar ratio) at 1373 K for 10 h according to the reported method.[58,67] The powdery potassium hexaniobate was then subjected to intercalation of three alkylammonium ions. For the intercalation of dodecyl- or hexylammonium ions, the niobate was allowed to react with an aqueous solution of a chloride salt of the alkylammonium ions with K:N atomic ratio of 1:8 at 333 K for 2 weeks, followed by washing with water and drying under ambient conditions.[58,64,65] For the intercalation of butylammonium ions, the reaction was carried out under the same conditions as described above but the reaction period was 6 weeks, and the product was thoroughly washed with water, once rinsed with acetone, and dried under ambient conditions.[58] The niobate samples intercalated with dodecyl-, hexyl-, and butylammonium ions are designated as $C_{12}N-Nb_6O_{17}$, $C_6N-Nb_6O_{17}$, and $C_4N-Nb_6O_{17}$, respectively.

The intercalation of alkylammonium ions was confirmed by powder X-ray diffraction (XRD, Figure S1 of the Supporting Information). The XRD patterns indicated the expansion of the basal spacings compared with $K_4Nb_6O_{17}$, and the expanded spacings were in agreement with the previous papers on the intercalation of alkylammonium ions.[58,64,65] The basal spacings indicated that all of the products incorporated the alkylammonium ions into both the two types of the interlayer spaces of hexaniobate.[58] The amount of intercalated alkylammonium ions was estimated with thermogravimetry. The alkylammonium:Nb molar ratio was 3.5:6, 3.3:6, and 3.2:6 for $C_{12}N-Nb_6O_{17}$, $C_6N-Nb_6O_{17}$, and $C_4N-Nb_6O_{17}$, respectively; namely, the rate of cation exchange was slightly larger for the longer-chain alkylammonium species. Water vapor adsorption isotherms of the alkylammonium-intercalated niobate were obtained at 298 K by a BEL Japan BELSORP 18-Plus automatic vapor adsorption apparatus with the previously reported method.[65]

Preparation and Characterization of Emulsions. Water−toluene emulsions were prepared by homogenizing a mixture of water, toluene, and the alkylammonium-intercalated niobate powders with a rotating speed of 20000 rpm for 5 min with an IKA T25 Ultra Turrax homogenizer. The temperature was kept to be 283 K with a water bath. Concentration of the intercalated niobate (c_S, in g L^{-1}) and volume fraction of water (ϕ_W) were examined as the variables while the total amount of the solvents was 15 mL. An emulsion was judged as stable when the emulsified state was kept more than 1 day, whereas it was recognized as unstable if demulsified within 24 h. We note that all of the emulsions judged as stable in the present study were kept for more than a month. The type of emulsions, w/o or o/w, was evaluated by the dilution test. The prepared emulsions were observed with an Olympus BX-51 optical microscope.

Adsorption and Photocatalytic Decomposition of Porphyrin Dyes. Adsorption and photocatalytic decomposition of organic dyes by the $C_{12}N-Nb_6O_{17}$ and $C_6N-Nb_6O_{17}$ particles in the emulsions were examined for two porphyrin species: water-soluble 5,10,15,20-tetrakis(1-methylpyridinium-4-yl) porphine (H_2TMPyP^{4+}) and toluene-soluble tetraphenylporphine (TPP). The dyes were first dissolved into the good solvent with the concentration of 10 μmol L^{-1}, and then subjected to emulsification with the poor solvent and the niobate powders. The ϕ_W and c_S values were set to 0.5 and 2 g L^{-1}, respectively. The prepared emulsions were kept in the dark for a day. Fluorescence microscope observations of the dye-including emulsions were carried out with an Olympus BX2-FL-1 system using a U-MSWB2 mirror unit. Adsorption of the porphyrin species onto the powders in the emulsions was evaluated with visible spectra of the supernatant obtained by removing the niobate powders with centrifugation (20 000 rpm, 10 min).

For the photocatalytic decomposition, the porphyrin-containing emulsions of 3 mL were irradiated in a quartz cell (1 cm path length) with an Ushio SX-U1500XQ Xe lamp. A Kenko U-340 UV-band-pass filter was used to irradiate the sample only with UV light (260−390 nm). Decomposition of the dyes was monitored by visible diffuse reflectance spectroscopy using a Shimadzu UV-2450 spectrophotometer equipped with an integrating sphere.

RESULTS AND DISCUSSION

All of the alkylammonium-intercalated niobates prepared in the present study — $C_{12}N-Nb_6O_{17}$, $C_6N-Nb_6O_{17}$, and $C_4N-Nb_6O_{17}$ — form Pickering emulsions at appropriate ϕ_W and c_S values. The emulsification behavior is somewhat different depending on the intercalated alkylammonium species. On the

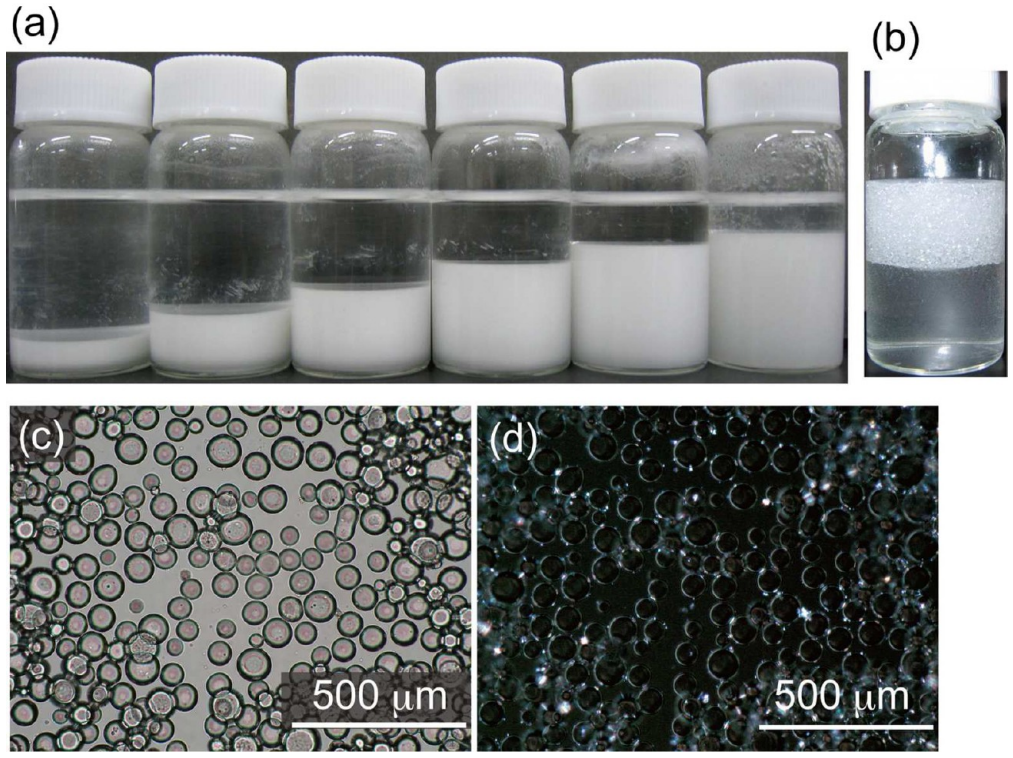

Figure 1. Photographs of the (a) w/o emulsions prepared with C_6N–Nb_6O_{17} (c_S = 2 g L^{-1}, ϕ_W = 0.1, 0.2, 0.3, 0.4, 0.5, 0.6 from left to right) and (b) instable o/w emulsion (c_S = 0.5 g L^{-1}, ϕ_W = 0.7), and optical microscope images of the w/o emulsion (c) without and (d) with crossed polarizers (c_S = 2 g L^{-1}, ϕ_W = 0.5).

contrary, unmodified $K_4Nb_6O_{17}$ does not stabilize emulsions at all.

Emulsions with C_6N–Nb_6O_{17}. Figure 1a shows a photograph of typical samples obtained with C_6N–Nb_6O_{17}. The samples consist of emulsion (in lower part of the vials) and pure toluene (upper part) phases, and the emulsion type is all w/o. Optical microscope images of a typical emulsion sample with and without crossed polarizers shown in Figures 1c and d indicate that water droplets are dispersed in toluene with birefringence at the droplet edges. Because of optical anisotropy of the $K_4Nb_6O_{17}$ crystallites,[67] the birefringence is ascribed to the presence of the C_6N–Nb_6O_{17} particles at the droplet edges; hence, the samples are Pickering emulsions.

We draw a phase diagram by examining the emulsification behavior of C_6N–Nb_6O_{17} with various ϕ_W and c_S values. Figure 2 shows the obtained diagram. Stable w/o emulsification is attained in the region of ϕ_W < 0.8 and c_S > 1 g L^{-1}. Emulsification is also possible down to c_S = 0.2 g L^{-1} if ϕ_W < 0.2. Instable w/o emulsions form in most of the other region. However, instable o/w emulsions also form in a limited region of large water content (ϕ_W = 0.6–0.9, c_S < 0.5 g L^{-1}); typical sample appearance is shown in Figure 1b. This is evidence for the phase inversion that is observed for the particle emulsifiers with the surface property near the border of hydrophobic and hydrophilic. The phase behavior indicates that C_6N–Nb_6O_{17} works as a moderately hydrophobic particle emulsifier.

Volume fraction of the emulsion phase in the samples gives additional information. Figure 3 shows volume fraction of the emulsion phase with different ϕ_W at c_S = 2 g L^{-1}. The fraction of the emulsion phase becomes large as ϕ_W increases at a constant c_S. This is usual behavior of Pickering emulsions.

Emulsions with $C_{12}N$–Nb_6O_{17}. The emulsification behavior of $C_{12}N$–Nb_6O_{17} is similar to that of C_6N–Nb_6O_{17}.

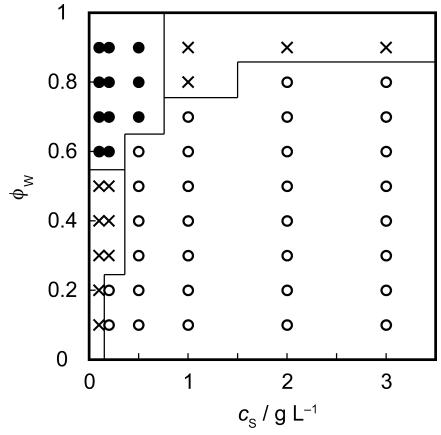

Figure 2. Phase diagram of the emulsions with C_6N–Nb_6O_{17}. Open circles, filed circles, and crosses mean stable w/o emulsion, instable w/o emulsion, and instable o/w emulsion phases, respectively.

Photographs of typical samples, Figure 4a, show that stable w/o emulsions are obtained in the lower part of the vials with the upper toluene phases. These behaviors are essentially the same as those observed for the C_6N–Nb_6O_{17} system. Volume fraction of the emulsion phase depends on the ϕ_W value similarly to the C_6N–Nb_6O_{17} system (Figure 3). Optical microscope images of an emulsion, Figures 4b and c, indicate the location of niobate particles evidenced by the birefringence both at the droplet edges and in the continuous liquid (toluene). This is different from the C_6N–Nb_6O_{17} system where the niobate particles are almost located at the droplet edges.

The optical microscopy also gives the information of the surface coverage of the emulsion droplets. We obtained a

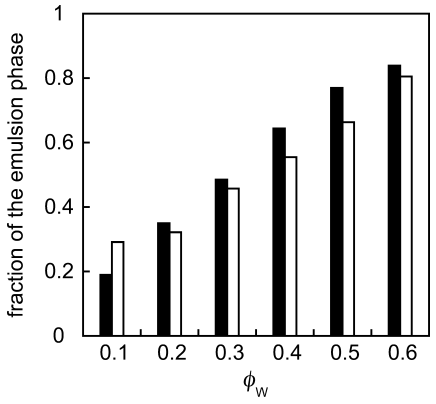

Figure 3. Volume fraction of the emulsion phase in the C_6N–Nb_6O_{17} (black bars) and $C_{12}N$–Nb_6O_{17} (white bars) samples with $0.1 < \phi_W < 0.6$ at a constant c_S of 2 g L^{-1}.

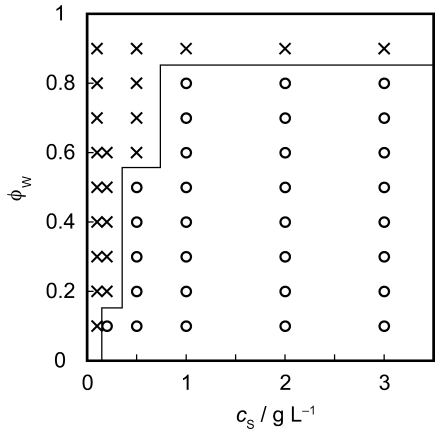

Figure 5. Phase diagram of the emulsions with $C_{12}N$–Nb_6O_{17}. Open circles and crosses mean stable w/o emulsion and instable w/o emulsion phases, respectively.

polarized microscope image of an emulsion droplet edge with a large magnification (c_S = 2 g L^{-1}, ϕ_W = 0.5) (see Figure S2 in the Supporting Information). The image indicates that the droplet is fully covered with the birefringent niobate particles. The thickness of the birefringent periphery is estimated as several micrometers, corresponding to the stacking of several thousands niobate layers. The particle thickness is in harmony with that can be estimated from a scanning electron microscope image of the $C_{12}N$–Nb_6O_{17} particles reported in a previous paper.[68]

The phase diagram of the $C_{12}N$–Nb_6O_{17} system, shown in Figure 5, is almost the same as that of the C_6N–Nb_6O_{17} system. Stable w/o emulsion forms in the region of $\phi_W < 0.8$ and $c_S > 1$ g L^{-1}, and $\phi_W < 0.2$ at c_S = 0.2 g L^{-1}. Only instable w/o emulsion forms in the other region; the phase inversion to o/w emulsion is not observed, which is different from the C_6N–Nb_6O_{17} system. The differences between the C_6N–Nb_6O_{17} and $C_{12}N$–Nb_6O_{17} systems are ascribed to more hydrophobic character of the $C_{12}N$–Nb_6O_{17} particles as rationalized by intercalation of the longer-chain $C_{12}N$ species, compared with the C_6N–Nb_6O_{17} particles.

The hydrophobic character of the $C_{12}N$–Nb_6O_{17} particles is also evidenced by the water vapor adsorption. Figure 6 compares the adsorption isotherms of the alkylammonium-intercalated niobate examined in the present study. Although all of the isotherms are classified into type II of the IUPAC definition indicating affinity for water,[69] the amounts of adsorbed water are in the order of $C_{12}N$–Nb_6O_{17} < C_6N–Nb_6O_{17} < C_4N–Nb_6O_{17}. This indicates that $C_{12}N$–Nb_6O_{17} is

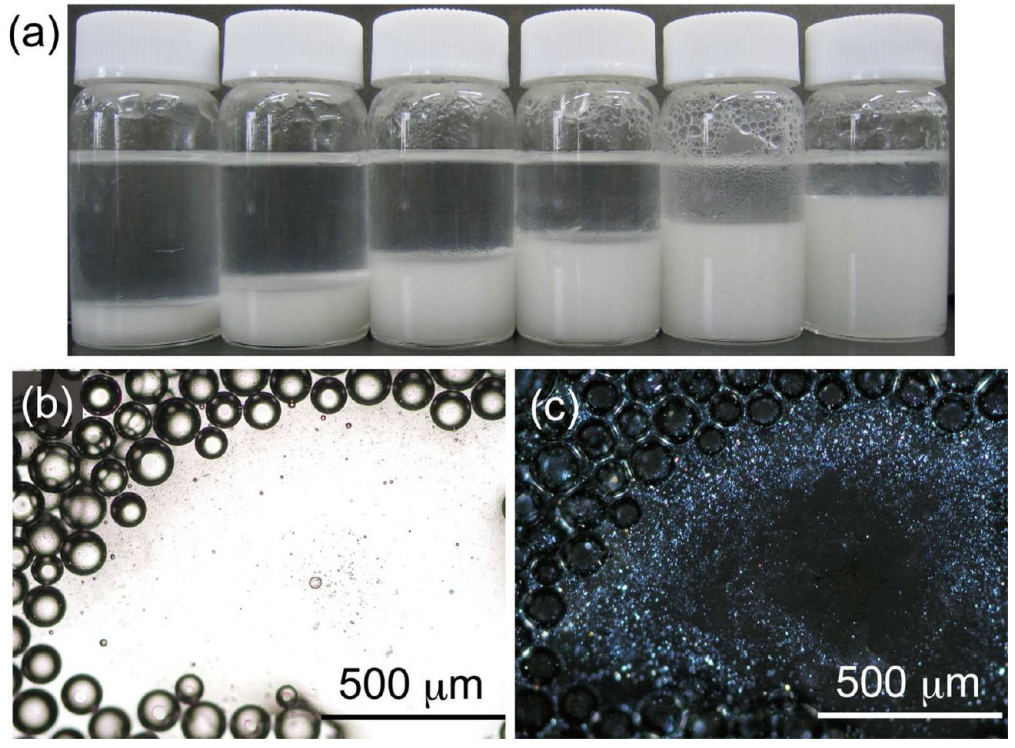

Figure 4. (a) Photographs of the w/o emulsions prepared with $C_{12}N$–Nb_6O_{17} (c_S = 2 g L^{-1}, ϕ_W = 0.1, 0.2, 0.3, 0.4, 0.5, 0.6 from left to right), and optical microscope images of the emulsion (c) without and (d) with crossed polarizers (c_S = 2 g L^{-1}, ϕ_W = 0.5).

dx.doi.org/10.1021/am300987x | ACS Appl. Mater. Interfaces 2012, 4, 4338–4347

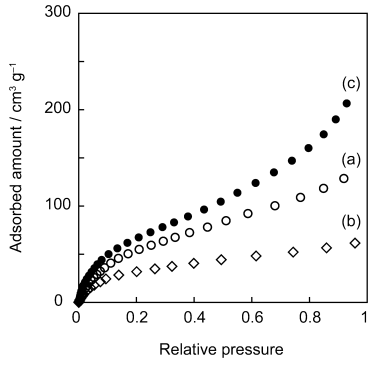

Figure 6. Water vapor adsorption isotherms for (a) $C_6N-Nb_6O_{17}$, (b) $C_{12}N-Nb_6O_{17}$, and (c) $C_4N-Nb_6O_{17}$.

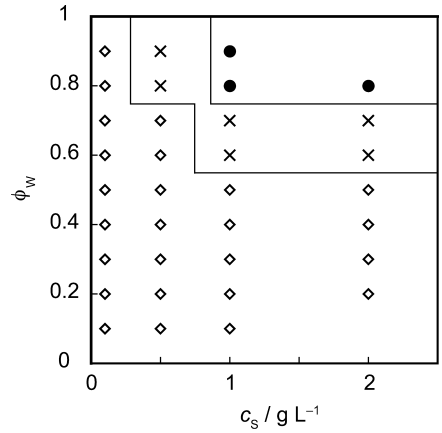

Figure 8. Phase diagram of the emulsions with $C_4N-Nb_6O_{17}$. Squares, crosses, and filled circles mean not emulsified, instable o/w emulsion, and stable o/w emulsion phases, respectively.

the most hydrophobic and $C_4N-Nb_6O_{17}$ is the most hydrophilic, agreeing with the order of hydrophobicity expected from the chain length of the intercalated alkylammonium species.

Emulsions with $C_4N-Nb_6O_{17}$. In contrast to $C_6N-Nb_6O_{17}$ and $C_{12}N-Nb_6O_{17}$, the emulsification behavior of $C_4N-Nb_6O_{17}$ is characteristic to that of hydrophilic particles. The $C_4N-Nb_6O_{17}$ particles generate o/w emulsions. Photograph of the samples emulsified with $C_4N-Nb_6O_{17}$ shown in Figure 7 indicates that the emulsions are present at the upper parts of the vials with turbid water phases of the lower parts. The turbidity of the water phase is due to the distribution of the niobate particles in the continuous phase as well as the droplet interface.

The phase diagram shown in Figure 8 indicates that the $C_4N-Nb_6O_{17}$ particles stabilize o/w emulsions in the rather restricted region of $\phi_W > 0.6$ and $c_S > 1$ g L^{-1}, and that w/o emulsions are not obtained. Macroscopically separated oil and water phases, where the niobate particles are suspended in the aqueous phase, are obtained outside the emulsification region (see Figure 7). Such behavior of the $C_4N-Nb_6O_{17}$ sample is explained with the most hydrophilic nature of this sample compared with the others because of the intercalation of short-chain C_4N cations as indicated by the water adsorption isotherm; hydrophilic particles stabilize o/w emulsions. However, hydrophilicity of the $C_4N-Nb_6O_{17}$ particles is not ideal as an efficient emulsifier because the niobate particles are not only adsorbed at the water–toluene interface but also dispersed in the aqueous phase.

Adsorption of Porphyrins Added to the Emulsions. We have examined adsorption of water- and oil-soluble porphyrins onto the $C_6N-Nb_6O_{17}$ and $C_{12}N-Nb_6O_{17}$ particles forming the w/o emulsions ($c_S = 2$ g L^{-1}, $\phi_W = 0.5$). The water-soluble cationic porphyrin, H_2TMPyP^{4+}, is adsorbed by the particles because the niobate layers are negatively charged. For $C_6N-Nb_6O_{17}$, visible spectra of the water and toluene supernatants after the removal of the emulsifier particles from the emulsion indicate that H_2TMPyP^{4+} cations do not reside in the aqueous phase (see Figure S3 in the Supporting Information); hence, the porphyrin molecules are all adsorbed onto the $C_6N-Nb_6O_{17}$ particles. Visible diffuse reflectance spectrum of the porphyrin-containing emulsion shown in Figure 9 exhibits the Soret band of the H_2TMPyP^{4+} species at 426 nm, being red-shifted by 5 nm from that of an aqueous H_2TMPyP^{4+} solution. The spectral shift supports the adsorption of porphyrin molecules onto the niobate particles.[70−72] The adsorption of porphyrin is also evidenced by fluorescence optical microscopy. Figure 10a shows a typical microscope image of the emulsion with $C_6N-Nb_6O_{17}$ containing H_2TMPyP^{4+}. It exhibits red emission of H_2TMPyP^{4+} from the water–oil interface, where the niobate particles are located, of the emulsion droplets.

The $C_{12}N-Nb_6O_{17}$ system shows somewhat different behavior. The H_2TMPyP^{4+} molecules are not completely adsorbed by the niobate particles but present in the water phase as dissolved species, which is indicated by visible spectrum of the water phase from which the emulsifier is removed (see Figure S3 in the Supporting Information), although the amount of H_2TMPyP^{4+} species is less than 1/100 (in molar ratio) that of alkylammonium ions, i.e., all of the H_2TMPyP^{4+} molecules can be adsorbed. However, fluorescence microscope image of the porphyrin-containing emulsion shown in Figure 10b

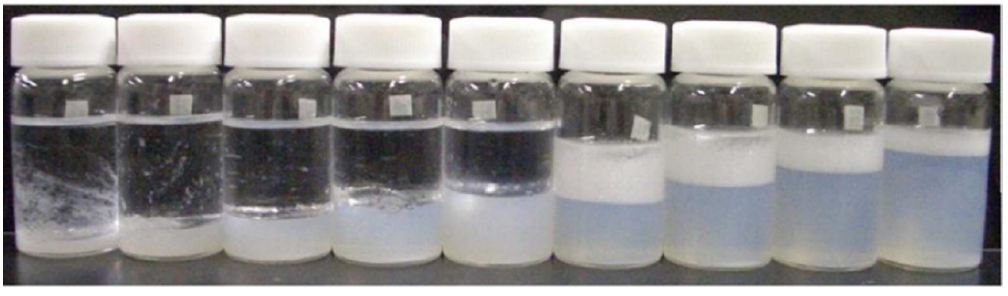

Figure 7. (a) Photographs of the o/w emulsions and suspensions prepared with $C_4N-Nb_6O_{17}$ ($c_S = 1$ g L^{-1}, $\phi_W = 0.1$, 0.2, 0.3, 0.4, 0.5, 0.6, 0.7, 0.8, 0.9 from left to right).

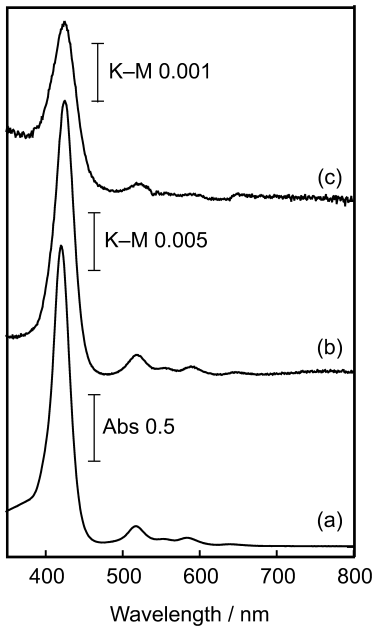

Figure 9. Visible spectra of (a) a 10 μmol L^{-1} aqueous H_2TMPyP^{4+} solution (transmission spectrum), and the w/o emulsions containing 10 μmol L^{-1} H_2TMPyP^{4+} stabilized with (b) $C_6N-Nb_6O_{17}$ and (c) $C_{12}N-Nb_6O_{17}$ (c_S = 2 g L^{-1}, ϕ_W = 0.5, diffuse reflectance spectra).

indicates intense emission from the droplet edge. Thus, the $C_{12}N-Nb_6O_{17}$ particles at the water–toluene interface adsorb the porphyrin molecules. This is also supported by the visible diffuse reflectance spectrum of the emulsion (Figure 9c) showing the Soret band at the position same as that of the $C_6N-Nb_6O_{17}$ system. The fluorescence microscope image also shows that only the niobate particles at the water–oil interface emit; emission from the toluene continuous phase is not observed although the polarized optical microscope image (Figure 4c) shows the location of the niobate particles inside the toluene continuous phase. This indicates that the particles distributed in the oil phase do not contribute to the adsorption of the dye dissolved in the aqueous phase, which is rationalized by little migration of the water-soluble H_2TMPyP^{4+} molecules into the toluene phase.

On the other hand, the oil-soluble porphyrin, TPP, is little adsorbed by both of the $C_6N-Nb_6O_{17}$ and $C_{12}N-Nb_6O_{17}$ particles. Fluorescence optical microscope image shown in Figure 10 exhibits emission from continuous toluene phase but not from the edge of emulsion droplets with $C_{12}N-Nb_6O_{17}$ with contrary to the microscope images of the H_2TMPyP^{4+}-containing emulsions. Diffuse reflectance spectrum of the emulsion with the $C_6N-Nb_6O_{17}$ particles shown in Figure 11 indicates the Soret absorption band of TPP at 419 nm, which is the same position as that of the porphyrin dissolved in toluene. Hence, the TPP molecules are not adsorbed onto the niobate particles at the water–toluene interface but stay inside the toluene phase. This is explained by electrical neutrality and hydrophobicity of the TPP species, which thus does not have specific driving force of adsorption between the electrically charged niobate layers.

Photocatalytic Decomposition of the Porphyrins in the Emulsions. Photocatalytic decomposition of the porphyrins added to the emulsions has been examined for the w/o emulsions with $C_6N-Nb_6O_{17}$ (c_S = 2 g L^{-1}, ϕ_W = 0.5), where the location of the porphyrin molecules is almost uniquely

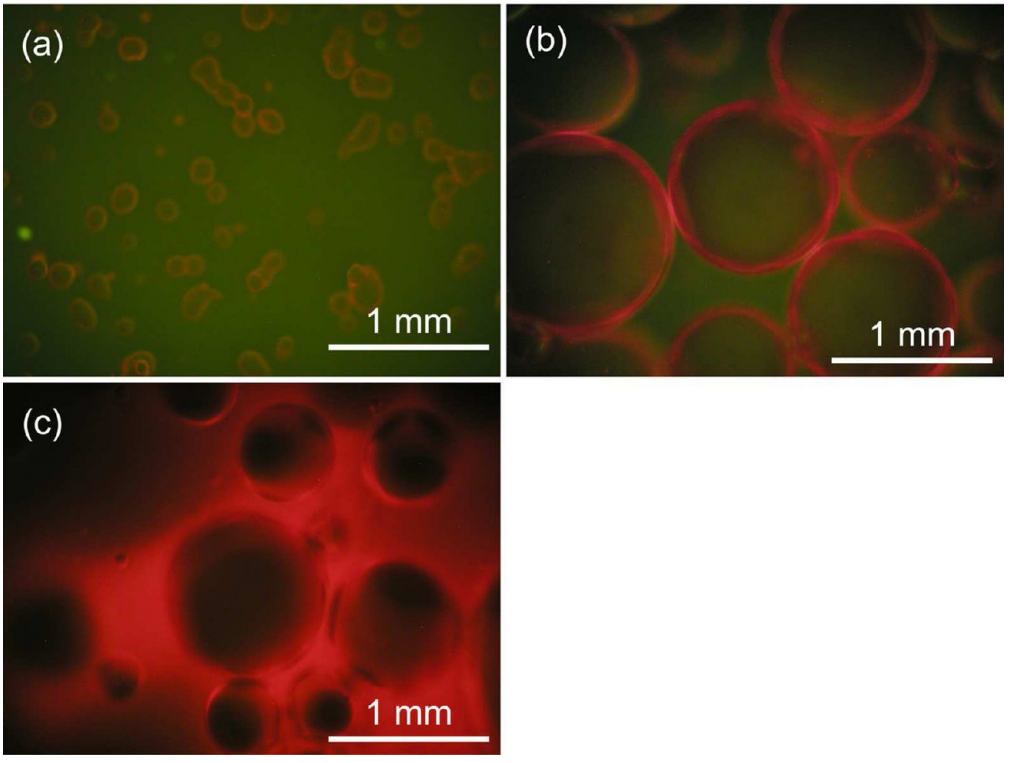

Figure 10. Fluorescence microscope images of the w/o emulsions (c_S = 2 g L^{-1}, ϕ_W = 0.5) containing H_2TMPyP^{4+} stabilized with (a) $C_6N-Nb_6O_{17}$ ([H_2TMPyP^{4+}] = 5 μmol L^{-1}) and (b) $C_{12}N-Nb_6O_{17}$ ([H_2TMPyP^{4+}] = 2.5 μmol L^{-1}), and w/o emulsion (c_S = 2 g L^{-1}, ϕ_W = 0.5) containing TPP stabilized with (c) $C_{12}N-Nb_6O_{17}$ ([TPP] = 1.5 μmol L^{-1}).

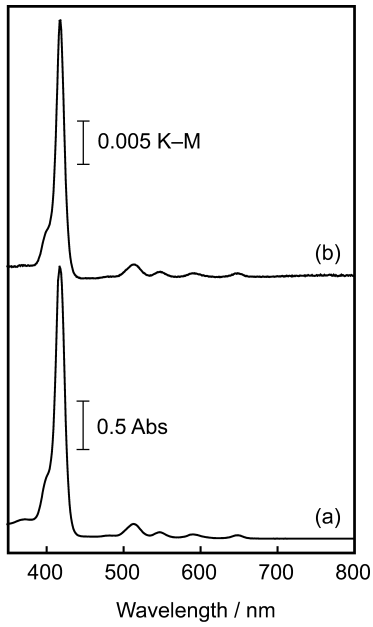

Figure 11. Visible spectra of (a) a 10 μmol L^{-1} TPP toluene solution (transmission spectrum), and (b) the w/o emulsion containing 10 μmol L^{-1} TPP stabilized with C_6N–Nb_6O_{17} (c_S = 2 g L^{-1}, ϕ_W = 0.5, diffuse reflectance spectrum).

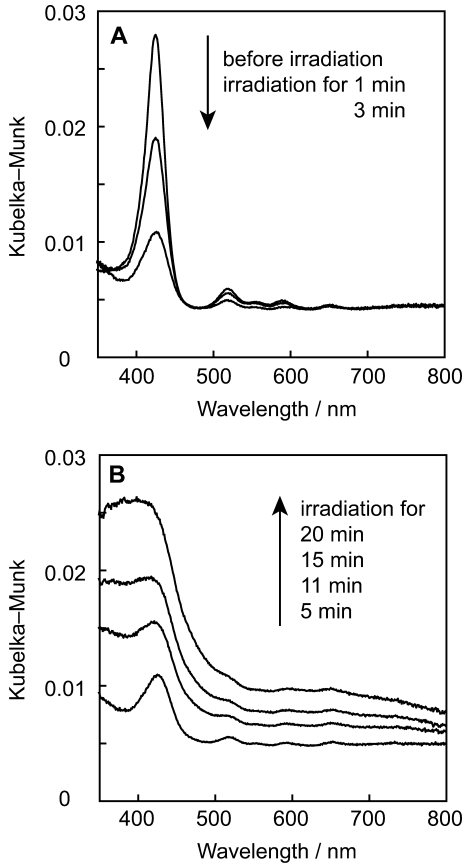

Figure 12. Visible diffuse reflectance spectra of the w/o emulsion containing 10 μmol L^{-1} H_2TMPyP^{4+} stabilized with C_6N–Nb_6O_{17} (c_S = 2 g L^{-1}, ϕ_W = 0.5) (A) before and after the irradiation for 1–3 min and (B) after the irradiation for 5–20 min.

defined. When H_2TMPyP^{4+} is added to the emulsion, it is decomposed with UV irradiation as monitored by the disappearance of the Soret band at 426 nm in the diffuse reflectance spectra of the emulsion shown in Figure 12A. The band intensity rapidly decreases with the irradiation. On the other hand, the visible diffuse reflectance spectra of the sample irradiated for 5–30 min, shown in Figure 12B, exhibit a very broad absorption band extending over the measured wavelength region with peaks around 400 and 650 nm. These bands are assigned to a reduced (lower-valent) Nb species in the niobate particles.[73−75] Organic species intercalated in or adsorbed on the layered niobate has been reported to act as a sacrificial donor to consume the positive holes in the niobate layers generated by photoexcitation of the semiconductor oxide;[60,76] and thus the Nb species in the niobate layers is reduced.

TPP molecules added to the emulsion are also photodecomposed. Figure 13 shows diffuse reflectance spectra of the emulsion containing TPP molecules before and after the UV irradiation. A rapid decrease in the intensity of the Soret band and gradual growth of the broad absorption band assigned to the lower-valence Nb species are observed as in the case of the H_2TMPyP^{4+}-containing emulsion. The redox potentials of the porphyrins at the ground state are +1.11 and +1.00 V (vs SCE) for H_2TMPyP^{4+} and TPP, respectively.[77,78] Also, those at the excited state are −0.73 and −0.89 V for H_2TMPyP^{4+} and TPP, respectively. Thus, both of the porphyrins can be oxidized by the positive holes of the niobate whose valence band level is estimated as +2.52 V.[79] These values explain the similar decomposition behavior of H_2TMPyP^{4+} and TPP. However, the decomposition of TPP is somewhat slower than H_2TMPyP^{4+} on the basis of the comparison of Figures 12A and 13A. This difference suggests an effect of the location of porphyrin molecules. Although the H_2TMPyP^{4+} molecules adsorbed on the photocatalytically active C_6N–Nb_6O_{17} particles are decomposed fast, the TPP species not located on the photocatalyst but dissolved in the liquid phase reacts somewhat slowly.

The emulsions are stable during the photocatalytic decomposition of porphyrins under our experimental conditions. Figure 14 shows photograph of the TPP-containing w/o emulsion stabilized with C_6N–Nb_6O_{17} (c_S = 2 g L^{-1}, ϕ_W = 0.5) before and after the irradiation for 21 min. Although the emulsion turned pale green after the irradiation due to the formation of the lower-valence niobate species as mentioned above, appearance of the irradiated emulsion is almost the same as that before the irradiation, and the volume fraction of the emulsion phase is reduced only a little with the irradiation. IR spectra of the powder of C_6N–Nb_6O_{17} recovered from the TPP-containing emulsion shown in Figure S4 of the Supporting Information indicate that the absorption bands at around 2900 cm^{-1} and 1700–1300 cm^{-1} due to the organic species still clearly appear after the reaction although that the band profile changes because of the decomposition of the TPP molecules. The intercalated hexylammonium ions would also be decomposed in part.

The photocatalytic decomposition of TPP species is greatly suppressed in the toluene suspension of C_6N–Nb_6O_{17} powders without emulsification in contrast to the effective decomposition in the Pickering emulsion. Figure S5 of the Supporting Information compares the visible spectra of TPP before and after the irradiation for 30 min. Although the TPP concentration (10 μmol L^{-1}) is the same as that of the emulsion system and the amount of C_6N–Nb_6O_{17} is larger (c_S

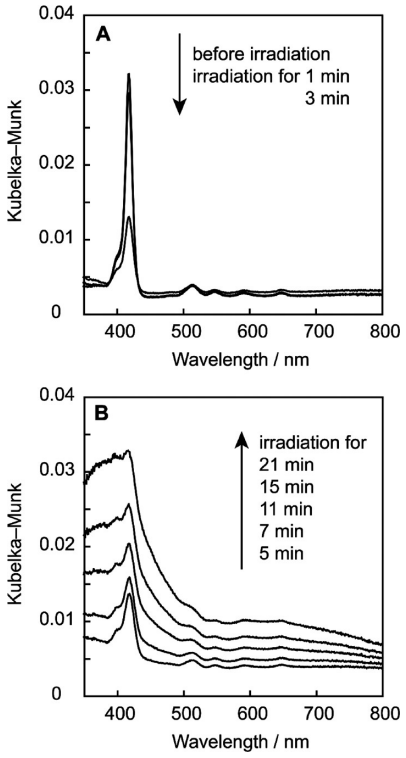

Figure 13. Visible diffuse reflectance spectra of the w/o emulsion containing 10 μmol L^{-1} TPP stabilized with C_6N–Nb_6O_{17} (c_S = 2 g L^{-1}, ϕ_W = 0.5) (A) before and after the irradiation for 1–3 min and (B) after the irradiation for 5–21 min.

Figure 14. Photographs of the w/o emulsion samples containing 10 μmol L^{-1} TPP stabilized with C_6N–Nb_6O_{17} (c_S = 2 g L^{-1}, ϕ_W = 0.5) (a) before and (b) after the irradiation for 21 min.

~ 4 g L^{-1}), the TPP concentration little decreased with the irradiation. This result clarifies the benefit of the photocatalytic reaction in the emulsions.

When H_2TMPyP^{4+} and TPP molecules are both added to the w/o emulsion with C_6N–Nb_6O_{17}, the niobate particles simultaneously photodecompose both of the porphyrin species. In this case, diffuse reflectance spectra of the emulsion containing the binary porphyrin species shown in Figure 15

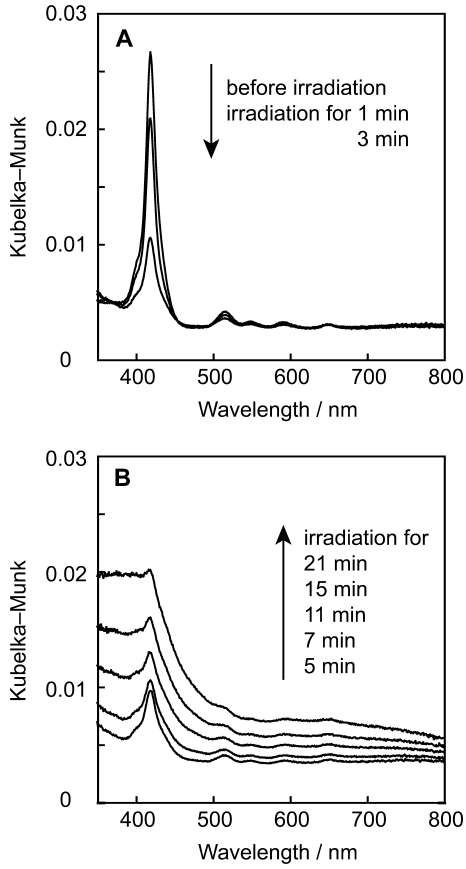

Figure 15. Visible diffuse reflectance spectra of the w/o emulsion containing 10 μmol L^{-1} H_2TMPyP^{4+} and TPP stabilized with C_6N–Nb_6O_{17} (c_S = 2 g L^{-1}, ϕ_W = 0.5) (A) before and after the irradiation for 1–3 min and (B) after the irradiation for 5–21 min.

indicate disappearance of TPP in toluene upon UV irradiation because of the absorption wavelength of the Soret band. At the same time, the niobate solid recovered from the emulsion by centrifugation shows that the characteristic Soret absorption band of the H_2TMPyP^{4+} molecules observed before the irradiation vanishes in the sample after the irradiation, as shown in Figure 16. The results demonstrate that the organically modified niobate forming the Pickering emulsion nonselectively decompose organic dyes in the emulsion without distinction of their location.

CONCLUSIONS

In summary, amphiphilicity of the layered niobate is tuned by the intercalation of alkylammonium species with different chain length, which enables the niobate to systematically control its emulsification behavior in the mixtures of water and toluene. W/o and o/w Pickering emulsions are both obtained by appropriate choice of the alkylammonium species. The organically modified niobate located at the water–oil interface of the emulsion droplet adsorbs cationic porphyrins introduced into the aqueous phase but not electrically neutral hydrophobic one dissolved in the toluene phase. The photocatalytically active niobate particles decompose the porphyrin molecules in the emulsions without distinction of their location; the dye molecules adsorbed onto the niobate and dissolved in the

dx.doi.org/10.1021/am300987x | ACS Appl. Mater. Interfaces 2012, 4, 4338–4347

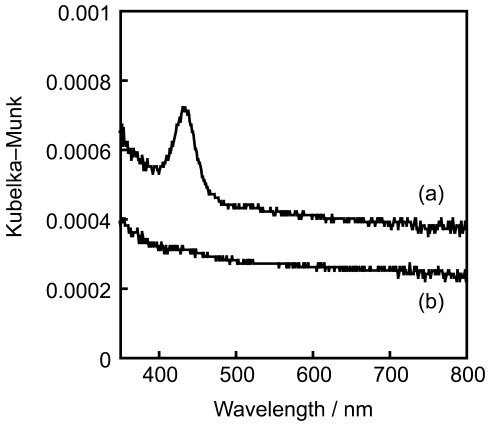

Figure 16. Visible diffuse reflectance spectra of the niobate powders recovered from the w/o emulsion containing 10 μmol L^{-1} H_2TMPyP^{4+} and TPP stabilized with C_6N–Nb_6O_{17} (c_S = 2 g L^{-1}, ϕ_W = 0.5) (a) before and (b) after the irradiation for 21 min.

organic phase are both decomposed. The results will be utilized for constructing novel photofunctional systems based on emulsion-based hierarchical structures.

■ ASSOCIATED CONTENT

Ⓢ Supporting Information

XRD patterns of C_6N–Nb_6O_{17}, $C_{12}N$–Nb_6O_{17}, and C_4N–Nb_6O_{17}. Magnified polarized optical microscope image of an emulsion droplet. Visible spectra of the supernatant aqueous phase of the emulsions obtained by centrifugation after the adsorption of H_2TMPyP^{4+}. IR spectra of C_6N–Nb_6O_{17} recovered from the TPP-containing emulsion. Visible spectra of a toluene solution of TPP before and after the irradiation of for 30 min in the presence of the powders of C_6N–Nb_6O_{17} without emulsification. This material is available free of charge via the Internet at http://pubs.acs.org/.

■ AUTHOR INFORMATION

Corresponding Author

*Phone & Fax: +81-93-884-3308. E-mail: nakato@che.kyutech.ac.jp.

Notes

The authors declare no competing financial interest.

■ ACKNOWLEDGMENTS

We thank Professor Toru Arai for telling us the redox potentials of porphyrins. This work was partly supported by Grants-in-Aid for Scientific Research on Innovative Areas ("Fusion Materials: Creative Development of Materials and Exploration of Their Function through Molecular Control", No. 23107511) from the Ministry of Education, Culture, Sports, Science and Technology, and for Scientific Research (B) (No. 24350107) and for challenging Exploratory Research (No. 24655198) from Japan Society for the Promotion of Science.

■ REFERENCES

(1) Ramsden, W. *Proc. R. Soc. London* **1903**, *72*, 156–164.
(2) Pickering, S. U. *J. Chem. Soc. Trans.* **1907**, *91*, 2001–2021.
(3) Binks, B. P. *Curr. Opin. Colloid Interface Sci.* **2002**, *7*, 21–41.
(4) Aveyard, R.; Binks, B. P.; Clint, J. H. *Adv. Colloid Interface Sci.* **2003**, *100–102*, 503–546.
(5) Böker, A.; He, J.; Emrick, T.; Russell, T. P. *Soft Matter* **2007**, *3*, 1231–1248.
(6) Glaser, N.; Adams, D. J.; Böker, A.; Krausch, G. *Langmuir* **2006**, *22*, 5227–5229.
(7) Walther, A.; Hoffmann, M.; Müller, A. H. E. *Angew. Chem., Int. Ed.* **2008**, *47*, 711–714.
(8) Kim, J.-W.; Lee, D.; Shum, H. C.; Weitz, D. A. *Adv. Mater.* **2008**, *20*, 3239–3243.
(9) Kim, S.-H.; Lee, S. Y.; Yang, S.-M. *Angew. Chem., Int. Ed.* **2010**, *49*, 2535–2538.
(10) Aveyard, R. *Soft Matter* **2012**, *8*, 5233–5240.
(11) Binks, B. P.; Desforges, A.; Duff, D. G. *Langmuir* **2007**, *23*, 1098–1106.
(12) Ghouchi Eskandar, N.; Simovic, S.; Prestidge, C. A. *Phys. Chem. Chem. Phys.* **2007**, *9*, 6426–6434.
(13) Binks, B. P.; Rodrigues, J. A.; Frith, W. J. *Langmuir* **2007**, *23*, 3626–3636.
(14) Binks, B. P.; Rodrigues, J. A. *Angew. Chem., Int. Ed.* **2007**, *46*, 5389–5392.
(15) Cui, Z.-G.; Yang, L.-L.; Cui, Y.-Z.; Binks, B. P. *Langmuir* **2009**, *26*, 4717–4724.
(16) Abend, S.; Bonnke, N.; Gutschner, U.; Lagaly, G. *Colloid Polym. Sci.* **1998**, *276*, 730–737.
(17) Thieme, J.; Abend, S.; Lagaly, G. *Colloid Polym. Sci.* **1999**, *277*, 257–260.
(18) Tsugita, A.; Takemoto, S.; Mori, K.; Yoneya, T.; Otani, Y. *J. Colloid Interface Sci.* **1983**, *95*, 551–560.
(19) Yamaguchi, M.; Kumano, Y.; Tobe, S. *Yukagaku (J. Jpn. Oil Chem. Soc.)* **1991**, *40*, 491–496.
(20) Lagaly, G.; Reese, M.; Abend, S. *Appl. Clay Sci.* **1999**, *14*, 83–103.
(21) Neuhäusler, U.; Abend, S.; Jacobsen, C.; Lagaly, G. *Colloid Polym. Sci.* **1999**, *277*, 719–726.
(22) Ashby, N. P.; Binks, B. P. *Phys. Chem. Chem. Phys.* **2000**, *2*, 5640–5646.
(23) Abend, S.; Lagaly, G. *Clay Miner.* **2001**, *36*, 557–570.
(24) Gu, G.; Zhou, Z.; Xu, Z.; Masliyah, J. H. *Colloids Surf. A* **2003**, *215*, 141–153.
(25) Binks, B. P.; Clint, J. H.; Whitby, C. P. *Langmuir* **2005**, *21*, 5307–5316.
(26) Yang, F.; Liu, S.; Xu, J.; Lan, Q.; Wei, F.; Sun, D. *J. Colloid Interface Sci.* **2006**, *302*, 159–169.
(27) Yang, F.; Quan, N.; Lan, Q.; Sun, D. *J. Colloid Interface Sci.* **2007**, *306*, 285–295.
(28) Yang, Y.; Liu, L.; Zhang, J.; Li, C.; Zhao, H. *Langmuir* **2007**, *23*, 2867–2873.
(29) Torres, L. G.; Iturbe, R.; Snowden, M. J.; Chowdhry, B. Z.; Leharne, S. A. *Colloids Surf. A* **2007**, *302*, 439–448.
(30) Bon, S. A. F.; Colver, P. J. *Langmuir* **2007**, *23*, 8316–8322.
(31) Bon, S. A. F.; Chen, T. *Langmuir* **2007**, *23*, 9527–9530.
(32) Wang, J.; Yang, F.; Li, C.; Liu, S.; Sun, D. *Langmuir* **2008**, *24*, 10054–10061.
(33) Whitby, C. P.; Fornasiero, D.; Ralston, J. *J. Colloid Interface Sci.* **2008**, *323*, 410–419.
(34) Nonomura, Y.; Suzuki, M. *Chem. Lett.* **2008**, *37*, 1196–1197.
(35) Nonomura, Y.; Kobayashi, N. *J. Colloid Interface Sci.* **2009**, *330*, 463–466.
(36) Guillot, S.; Bergaya, F.; de Azevedo, C.; Warmont, F.; Tranchant, J.-F. *J. Colloid Interface Sci.* **2009**, *333*, 563–569.
(37) Li, C.; Liu, Q.; Mei, Z.; Wang, J.; Xu, J.; Sun, D. *J. Colloid Interface Sci.* **2009**, *336*, 314–321.
(38) Wang, J.; Yang, F.; Liu, G.; Xu, J.; Sun, D. *Langmuir* **2009**, *26*, 5397–5404.
(39) Pardhy, N. P.; Budhlall, B. M. *Langmuir* **2010**, *26*, 13130–13141.
(40) Kim, J.; Cote, L. J.; Kim, F.; Yuan, W.; Shull, K. R.; Huang, J. *J. Am. Chem. Soc.* **2010**, *132*, 8180–8186.
(41) Song, X.; Yang, Y.; Liu, J.; Zhao, H. *Langmuir* **2011**, *27*, 1186–1191.
(42) Cui, Y.; Threlfall, M.; van Duijneveldt, J. S. *J. Colloid Interface Sci.* **2011**, *356*, 665–671.

(43) Gudarzi, M. M.; Sharif, F. *Soft Matter* **2011**, *7*, 3432−3440.
(44) Reger, M.; Sekine, T.; Okamoto, T.; Watanabe, K.; Hoffmann, H. *Soft Matter* **2011**, *7*, 11021−11030.
(45) Garcia, P. C.; Whitby, C. P. *Soft Matter* **2012**, *8*, 1609−1615.
(46) Hirsemann, D.; Shylesh, S.; De Souza, R. A.; Diar-Bakerly, B.; Biersack, B.; Mueller, D. N.; Martin, M.; Schobert, R.; Breu, J. *Angew. Chem., Int. Ed.* **2012**, *51*, 1348−1352.
(47) Tan, S.-Y.; Tabor, R. F.; Ong, L.; Stevens, G. W.; Dagastine, R. R. *Soft Matter* **2012**, *8*, 3112−3121.
(48) Zhang, J.; Li, L.; Wang, J.; Sun, H.; Xu, J.; Sun, D. *Langmuir* **2012**, *28*, 6769−6775.
(49) *Handbook of Layered Materials*; Auerbach, S. M.; Carrado, K. A.; Dutta, P. K., Eds.; Marcel Dekker: New York, 2004.
(50) Brugger, B.; Richtering, W. *Adv. Mater.* **2007**, *19*, 2973−2978.
(51) Kaiser, A.; Liu, T.; Richtering, W.; Schmidt, A. M. *Langmuir* **2009**, *25*, 7335−7341.
(52) Zhou, J.; Qiao, X.; Binks, B. P.; Sun, K.; Bai, M.; Li, Y.; Liu, Y. *Langmuir* **2011**, *27*, 3308−3316.
(53) Zhang, L.; Zhang, F.; Wang, Y.-S.; Sun, Y.-L.; Dong, W.-F.; Song, J.-F.; Huo, Q.-S.; Sun, H.-B. *Soft Matter* **2011**, *7*, 7375−7381.
(54) Domen, K.; Kudo, A.; Shinozaki, A.; Tanaka, A.; Maruya, K.; Onishi, T. *J. Chem. Soc., Chem. Commun.* **1986**, 356−357.
(55) Kudo, A.; Miseki, Y. *Chem. Soc. Rev.* **2009**, *38*, 253−278.
(56) Bizeto, M. A.; Shiguihara, A. L.; Constantino, V. R. L. *J. Mater. Chem.* **2009**, *19*, 2512−2525.
(57) Lagaly, G.; Beneke, K. *J. Inorg. Nucl. Chem.* **1976**, *38*, 1513−1518.
(58) Nakato, T.; Sakamoto, D.; Kuroda, K.; Kato, C. *Bull. Chem. Soc. Jpn.* **1992**, *65*, 322−328.
(59) Shinozaki, R.; Nakato, T. *Microporous Mesoporous Mater.* **2008**, *113*, 81−89.
(60) Nakato, T.; Edakubo, H.; Shimomura, T. *Microporous Mesoporous Mater.* **2009**, *123*, 280−288.
(61) Kiba, S.; Haga, J.; Hashimoto, S.; Nakato, T. *J. Nanosci. Nanotechnol.* **2010**, *10*, 8341−8348.
(62) Wang, Q.-Q.; Lin, B.-Z.; Xu, B.-H.; Li, X.-L.; Chen, Z.-J.; Pian, X.-T. *Microporous Mesoporous Mater.* **2010**, *130*, 344−351.
(63) Nakato, T.; Miyamoto, N. *J. Mater. Chem.* **2002**, *12*, 1245−1246.
(64) Nakato, T.; Miyashita, H.; Yakabe, S. *Chem. Lett.* **2003**, *32*, 72−73.
(65) Wei, Q.; Nakato, T. *Microporous Mesoporous Mater.* **2006**, *96*, 84−92.
(66) Nakato, T.; Hashimoto, S. *Chem. Lett.* **2007**, *36*, 1240−1241.
(67) Nassau, K.; Shiever, J. W.; Bernstein, J. L. *J. Electrochem. Soc.* **1969**, *116*, 348−353.
(68) Nakato, T.; Kameyama, M.; Wei, Q.; Haga, J.-i. *Microporous Mesoporous Mater.* **2008**, *110*, 223−231.
(69) Sing, K. S. W.; Everett, D. H.; Haul, R. A. W.; Moscou, L.; Pierotti, R. A.; Rouquerol, J.; Siemieniewska, T. *Pure Appl. Chem.* **1985**, *57*, 603−619.
(70) Nakato, T.; Iwata, Y.; Kuroda, K.; Kaneko, M.; Kato, C. *J. Chem. Soc., Dalton Trans.* **1993**, 1405−1409.
(71) Nakato, T.; Sugawara, J. *Bull. Chem. Soc. Jpn.* **2007**, *80*, 2451−2456.
(72) Takagi, S.; Eguchi, M.; Tryk, D. A.; Inoue, H. *J. Photochem. Photobiol. C* **2006**, *7*, 104−126.
(73) Wada, Y.; Morikawa, A. *Bull. Chem. Soc. Jpn.* **1987**, *60*, 3509−3513.
(74) Yao, J. N.; Loo, B. H.; Hashimoto, K. *Ber. Bunsen-Ges. Phys. Chem.* **1992**, *96*, 699−701.
(75) Carroll, E. C.; Compton, O. C.; Madsen, D.; Osterloh, F. E.; Larsen, D. S. *J. Phys. Chem. C* **2008**, *112*, 2394−2403.
(76) Nakato, T.; Yamada, Y.; Nakamura, M.; Takahashi, A. *J. Colloid Interface Sci.* **2011**, *354*, 38−44.
(77) Yui, T.; Tsuchino, T.; Akatsuka, K.; Yamauchi, A.; Kobayashi, Y.; Hattori, T.; Haga, M.; Takagi, K. *Bull. Chem. Soc. Jpn.* **2006**, *79*, 386−396.
(78) Yamada, H.; Imahori, H.; Nishimura, Y.; Yamazaki, I.; Ahn, T. K.; Kim, S. K.; Kim, D.; Fukuzumi, S. *J. Am. Chem. Soc.* **2003**, *125*, 9129−9139.
(79) Kim, Y. I.; Atherton, S. J.; Brigham, E. S.; Mallouk, T. E. *J. Phys. Chem.* **1993**, *97*, 11802−11810.